Journal of Catalysis **183,** 300–313 (1999)
Article ID jcat.1999.2413, available online at http://www.idealibrary.com on IDEAL®

Activity of Molybdenum Oxide Catalyst in the Dehydrogenation of *n*-Butane

M. E. Harlin,*,[1] L. B. Backman,* A. O. I. Krause,* and O. J. T. Jylhä†

*Department of Chemical Technology, Helsinki University of Technology, P.O. Box 6100, FIN-02015 HUT, Finland; and †Corporate Technology, Analytical Research, Neste Oy, P.O. Box 310, FIN-06101 Porvoo, Finland

Received September 8, 1998; revised December 21, 1998; accepted January 5, 1999

The catalytic properties of molybdenum oxide on alumina for the dehydrogenation of *n*-butane were studied at 560°C under atmospheric pressure. The rapidity of the technique used to analyze the reaction product (Fourier transform infra red gas analysis) made it possible to measure the activity in dehydrogenation and the changes in the reduction level of the catalyst during the first minutes on stream. The highest activity was obtained with a molybdenum content of 13%, which corresponds to a theoretical monolayer coverage on the γ-alumina. The oxidation state of the molybdenum active in the dehydrogenation was either Mo^{5+} or Mo^{4+}. Some catalyst samples were modified with magnesium to improve the selectivity to *n*-butenes. The highest yield of *n*-butenes achieved, 8%, was obtained with a Mg : Mo molar ratio of 1 : 1. The best selectivity to C_4 alkenes, 80%, was obtained with the highest content of magnesium, and was partly attributable to the formation of C_4 alkenes via the oxidative dehydrogenation reaction. The active oxidation state of molybdenum for dehydrogenation was not stable under the conditions used for testing, but was reduced to lower oxidation states, resulting in an increased selectivity to *n*-butane cracking and coke formation.

Key Words: **dehydrogenation; *n*-butane; molybdenum oxide; molybdates; catalysis.**

INTRODUCTION

The demand for light alkenes (C_3–C_5) is expected to increase during the coming years, because these hydrocarbons are essential building blocks of high-quality gasoline and diesel fuels and a variety of chemicals and polymers. The main supplies at present, from catalytic cracking units (FCC) and steam cracking units, are not sufficient to meet future requirements. In an attempt to meet the demand, a number of dehydrogenation units have already been commissioned. These units produce either isobutene (2-methyl propene) from isobutane to be used in MTBE (methyl *tert.*-butyl ether, 2-methoxy-2-methyl propane) production or propene from propane for polypropene production (1).

At this moment five dehydrogenation technologies are available for licensing, all of them relying on either chromium oxide or platinum catalysts (2). Chromium oxide catalysts deactivate rapidly and require frequent regeneration. Moreover, after regeneration a part of the chromium is in the oxidation state Cr^{6+} (3), which is carcinogenic. The platinum catalysts, in turn, are expensive and sensitive to various impurities, so that the feed and recycle streams have to be purified carefully. Platinum-based catalysts are typically very complicated, containing several components to ensure the stability of platinum under the severe conditions of commercial operations (1). An improved catalyst for the dehydrogenation of light paraffins would clearly be welcome.

In addition to chromium- and platinum-based catalysts, molybdenum (4–9), vanadium (10–12), palladium (13), zinc (14, 15), nickel (16), and gallium (17) compounds have been reported to be active in dehydrogenation. So far, however, none of these has performed at the activity and selectivity levels of the commercial catalysts.

Compared with chromium oxide, molybdenum oxide is far less harmful to the environment (18) and would be a feasible candidate to replace Cr. Molybdenum oxide on a silicon carbide carrier treated under reducing atmosphere has been shown to be active in dehydrogenation (4). The conversion of *n*-butane and the selectivity to C_4 alkenes obtained at 550°C were 20 and 80%, respectively. This catalyst also enhances the isomerization reaction of alkane at temperatures below 400°C. Besides the oxides, molybdenum in sulfided form has exhibited activity for the dehydrogenation reaction, with a selectivity of 64% to propene (5). One disadvantage of the sulfided system is that sulfur oxides are released during the regeneration and new sulfur compound is needed for the reactivation. So far, the greatest study has been made of the molybdenum oxides for use in oxidative dehydrogenation reactions (19).

The aim of our study was to evaluate in detail the catalytic performance of molybdenum oxide and estimate its potential for dehydrogenation. The activity in dehydrogenation was measured and the reduction and oxidation states of molybdenum oxide on the catalysts were characterized by

[1] To whom correspondence should be addressed. Fax: +358 9 451 2622. E-mail: harlin@polte.hut.fi.

0021-9517/99 $30.00

temperature-programmed reduction and X-ray photoelectron spectroscopy.

EXPERIMENTAL

Preparation of the Catalyst

Catalyst samples were prepared by incipient wetness impregnation on an alumina support. Prior to the impregnation, aluminum oxide extrudates (Akzo Nobel 000-1.5E) were crushed and sieved to a particle size of 0.3–0.5 mm and calcined at 600°C for 16 h with 5% oxygen in nitrogen (Aga, O_2 99.998%, N_2 99.999%).

The impregnation of molybdenum was accomplished with an aqueous solution of ammonium heptamolybdate, $(NH_4)_6Mo_7O_{24} \cdot 4H_2O$ (Merck, >99%). The pH of the molybdenum solution was between 3 and 4. After the impregnation step the sample was dried at 120°C for 8 h and calcined at 600°C for 6 h in a 5% O_2/N_2 mixture. For comparison one molybdenum catalyst was calcined for 6 h at 500°C.

Some samples were modified with magnesium: before molybdenum impregnation the alumina support was impregnated with a solution of magnesium nitrate, $Mg(NO_3)_2 \cdot 6H_2O$ (Merck, >99%). Drying and calcination steps were carried out in the same way as after the molybdenum impregnation.

Characterization of the Catalyst

The amounts of molybdenum and magnesium in the catalysts were measured by atomic absorption spectroscopy (AAS). Surface areas and pore volumes of the catalysts were determined with a Coulter Omnisorp 100CX (static volumetric method). The crystalline structure of the catalysts was studied by X-ray diffraction (XRD) analysis with a Phillips PW diffractometer MDP 1880 using Cu$K\alpha$ radiation.

The distribution of the metals in the support was studied by scanning electron microscopy (SEM) and energy-dispersive X-ray spectroscopy (EDS). The measurements were carried out with a JEOL JSM-840A scanning electron microscope equipped with a PGT Omega Light Element SiLi detector and fitted with IMIX version 6.860 software. Before the measurement the catalyst particles were embedded in epoxy resin, and cross sections of particles were cut with a glass-knife microtome. The samples were coated with carbon to prevent charging under the electron beam.

The reduction of the catalysts was studied by temperature-programmed reduction (TPR). The measurements were performed with an Altamira Instruments AMI-100 catalyst characterization system. The catalyst samples (50 mg) were dried at 130°C for 60 min with helium, calcined with 5% O_2/He at 560°C for 30 min, and cooled down to 30°C. During the reduction the samples were heated from 30 to 560 or 700°C at the rate of 5°C/min under 10% H_2 in argon (30 cm^3/min) and kept at this temperature for 30 min. The consumption of hydrogen was measured with a thermal conductivity detector (TCD).

To determine the oxidation states of molybdenum oxide on the catalysts some of the samples were characterized by X-ray photoelectron spectroscopy (XPS). Before the measurement, the samples were reduced in the Altamira AMI-100 system. The samples were dried under argon at 120°C for 8 h, calcined in 5% O_2/helium at 560°C for 2 h, reduced in 5% H_2/argon either at 560°C for 0, 5, 30, or 120 min or at 700°C for 120 min. After this, the samples were inertly transferred to a glove box and prepared for analysis under nitrogen atmosphere. Finally they were transferred to the XPS instrument under vacuum.

The XPS measurements were performed in an X-probe Model 101 spectrometer (Surface Science Instruments, VG Fisons) using a monochromatized Al$K\alpha$ X-ray source. A nickel grid and a flood gun were used to compensate sample charging. The background pressure during acquisition was better than 1×10^{-6} Pa (1×10^{-8} Torr). High resolution spectra of Mo 3*d*, Al 2*p*, O 1*s*, C 1*s*, and Mg 2*s* and a low-resolution survey spectrum were measured using a nominal spot size of 600 μm. The Al 2*p* line (74.5 eV) was used as a binding energy reference. The overlapping Mo 3*d* signals were deconvoluted using symmetrical Gaussian–Lorenzian (80/20) lines with the following constraints for all oxidation states: nonlinear Shirley background subtraction, Mo $3d_{5/2}$/Mo $3d_{3/2}$ intensity ratio of 1.45, and a doublet separation (Mo $3d_{5/2}$–Mo $3d_{3/2}$) of 3.13 eV.

Measurements of Catalyst Activity

The activities of the catalysts were measured in a fixed-bed microreactor. A catalyst load of 0.5 g was placed in a quartz reactor, and the temperature was measured in the middle of the bed. The catalyst was heated to the reaction temperature under 5% oxygen flow (Aga, O_2 99.5%, N_2 99.999%) and the reactor was then flushed with nitrogen (Aga, 99.999%) for 30 min before the first test at 560°C. The nitrogen used was purified with an Oxisorb (Messer Griesheim). The activities of the catalysts were compared at 560°C, at atmospheric pressure and with a weight hourly space velocity (WHSV) of 2 h^{-1}. The *n*-butane feed (Aga, 99.95%) was diluted with nitrogen, the molar ratio of nitrogen to *n*-butane being 9 : 1. Before some of the activity tests, the catalyst was reduced at 560°C with 5% hydrogen (Aga, 99.999%) for 5 or 30 min. Several reaction cycles could be performed with the same catalyst sample by regenerating the catalyst with diluted air between the cycles.

The products were analyzed with a Fourier transform infrared (FTIR) gas analyzer (Gasmet, Temet Instruments Ltd.). The spectra were measured in the wavenumber range 850–4000 cm^{-1} with a resolution of 8 cm^{-1} at a scanning rate of 10 scans/s. The cuvette (9 cm^3) was maintained at constant

temperature (175°C) and pressure (103 kPa). The analyzer was calibrated with pure compounds diluted with nitrogen: methane, ethane, ethene, propane, propene, i-butane, i-butene, *n*-butane, 1-butene, *cis*-2-butene, *trans*-2-butene, 1,3-butadiene, CO, CO_2, benzene, toluene, and water. The residuals in the fitting of the sample spectra with the set of calibration spectra were less than 5% of the sample spectra. The method of analyzing the reaction product has been discussed in detail elsewhere (20).

The amounts of water, carbon monoxide, and carbon dioxide formed in the reaction or during the reduction were measured, and the average oxidation state of molybdenum was calculated. It was possible to measure the amount of carbon oxides released during regeneration and to estimate the coke content of the catalyst.

The conversion and selectivity were calculated from the reaction product on the basis of the carbon balance: the total molar amount of carbon in the effluent was assumed to be equal to the molar amount of carbon in the *n*-butane fed to the reactor. The coke formed on the catalyst during the dehydrogenation test was usually neglected, but in some calculations the coke was included in the carbon balance. The total amount of *n*-butane fed to the reactor equals $C_{\mathrm{nb\,in}}$.

$$C_{\mathrm{nb\,in}} = \sum C_1 * \tfrac{1}{4} + \sum C_2 * \tfrac{2}{4} + \sum C_3 * \tfrac{3}{4} + \sum C_4 + C_6 * \tfrac{6}{4} + C_7 * \tfrac{7}{4}, \quad [1]$$

where C_i = molar amount of product containing *i* carbon in the reactor effluent, including hydrocarbons, CO, and CO_2. The conversion of *n*-butane equals X_{nb}.

$$X_{\mathrm{nb}} = 100 * \frac{C_{\mathrm{nb\,in}} - C_{\mathrm{nb\,out}}}{C_{\mathrm{nb\,in}}}, \quad [2]$$

where $C_{\mathrm{nb\,in}}$ = amount of *n*-butane fed to the reactor calculated according to Eq. [1] and $C_{\mathrm{nb\,out}}$ = amount of *n*-butane in the reactor effluent. The selectivity to a specific product, for example, *n*-butenes, $S_{\mathrm{nb=}}$, was calculated as

$$S_{\mathrm{nb=}} = 100 * \frac{C_{\mathrm{nb=}}}{C_{\mathrm{nb\,in}} - C_{\mathrm{nb\,out}}}, \quad [3]$$

where $C_{\mathrm{nb=}}$ = amount of *n*-butenes, 1-butene, *cis*-2-butene, and *trans*-2-butene in the reactor effluent. The selectivity S_{1-3} to cracked hydrocarbons was calculated from

$$S_{1-3} = 100 * \frac{C_{1m} * \tfrac{1}{4} + \sum C_2 * \tfrac{2}{4} + \sum C_3 * \tfrac{3}{4}}{C_{\mathrm{nb\,in}} - C_{\mathrm{nb\,out}}}, \quad [4]$$

where C_{1m} = amount of methane in the reactor effluent.

The yield of a specific product was obtained by multiplying the *n*-butane conversion by the corresponding selectivity.

RESULTS

Catalysts

The catalysts tested in the dehydrogenation of *n*-butane are listed in Table 1. The catalysts are designated according to the calculated amount of molybdenum impregnated on the catalyst. The amount of molybdenum measured by AAS is shown in Table 1. Assuming that a theoretical monolayer coverage of molybdenum oxide on alumina equals 5 Mo atoms/nm^2 (21, 22), the amount of 7–24 wt% Mo would equal 0.5–2 geometrical monolayers. After molybdenum impregnation all catalysts were calcined for 6 h at 600°C, except Mo13/500°C, which was calcined at 500°C.

The catalyst Mo13 was modified with 0.8–8.4 wt% magnesium to decrease the acidity of the alumina carrier and improve the selectivity to C_4 alkenes. The magnesium-modified catalysts are designated according to the molar ratio of the measured amount of magnesium to the measured amount of molybdenum in the catalyst; thus, the catalyst Mo13Mg0.8 contains magnesium with a molar ratio of magnesium to molybdenum of 0.8.

Table 1 also reports the surface area and total pore volume of the catalysts. When surface areas are calculated relative to the fraction of the alumina carrier of the catalysts, it can be seen that the addition of magnesium and 7 or 13 wt% molybdenum has little effect on the surface area. From this it can be assumed that the oxides were well dispersed on the support. The addition of 24% molybdenum, in turn, resulted in a decrease of 13% in the surface area of alumina, possibly due to blocking of pores during the formation of MoO_3 crystallites.

X-ray diffractograms of the molybdenum catalysts are presented in Fig. 1. Sample Mo13 contained crystalline MoO_3 when calcined at 500°C (Fig. 1a), but crystallites of

TABLE 1

Properties of the Catalysts

	Mo content (wt%)	Mg content (wt%)	Ratio Mg/Mo (mol/mol)	Surface area ($m^2/g_{catalyst}$)	Total pore volume ($cm^3/g_{catalyst}$)
Alumina	—	—		198	0.51
Mo13/500	13.3	—			
Mo7	6.8	—		200	0.38
Mo13	13.4	—		155	0.33
Mo24	24.1	—		110	0.26
Mg/alumina	—	2.8		188	0.45
Mo13Mg0.2	13.2	0.8	0.2		
Mo13Mg0.8	13.3	2.8	0.8	139	0.26
Mo13Mg0.9	12.1	2.8	0.9		
Mo13Mg1.2	12.9	4.0	1.2		
Mo13Mg1.9	13.5	6.7	1.9		
Mo13Mg2.9	12.8	8.4	2.9	157[a]	0.33[a]
				128	0.23

[a] After Mg impregnation.

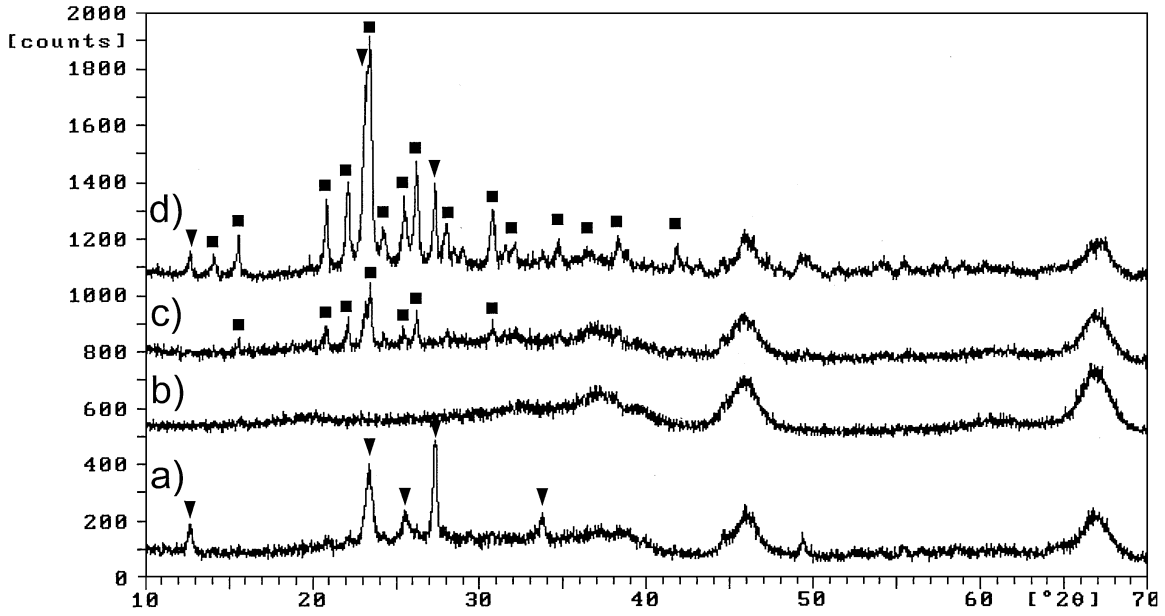

FIG. 1. X-ray diffractograms of the catalysts (a) Mo13/500, (b) Mo7, (c) Mo13, and (d) Mo24. The peaks are marked as (▼) MoO_3 and (■) $Al_2(MoO_4)_3$.

$Al_2(MoO_4)_3$ after calcination at 600°C (Fig. 1c). A further increase in the molybdenum content to 24% (Mo24) resulted in the formation of crystalline MoO_3. The diffraction pattern of γ-alumina can also be seen in diffractograms.

The diffraction pattern of samples containing molybdenum and magnesium is shown in Fig. 2. In these samples only catalysts with a small amount of magnesium (Mo13Mg0.2 and Mo13Mg0.8) contained crystalline $Al_2(MoO_4)_3$, while the samples with larger amounts (Mo13Mg0.8–Mo13Mg2.9) contained mainly crystalline $MgMoO_4$. Crystalline MgO and $MgAl_2O_4$ were not detected by XRD on these samples.

According to the elemental mapping of the SEM/EDS measurement of catalyst Mo13Mg0.8, molybdenum and magnesium were homogeneously distributed through the alumina particles.

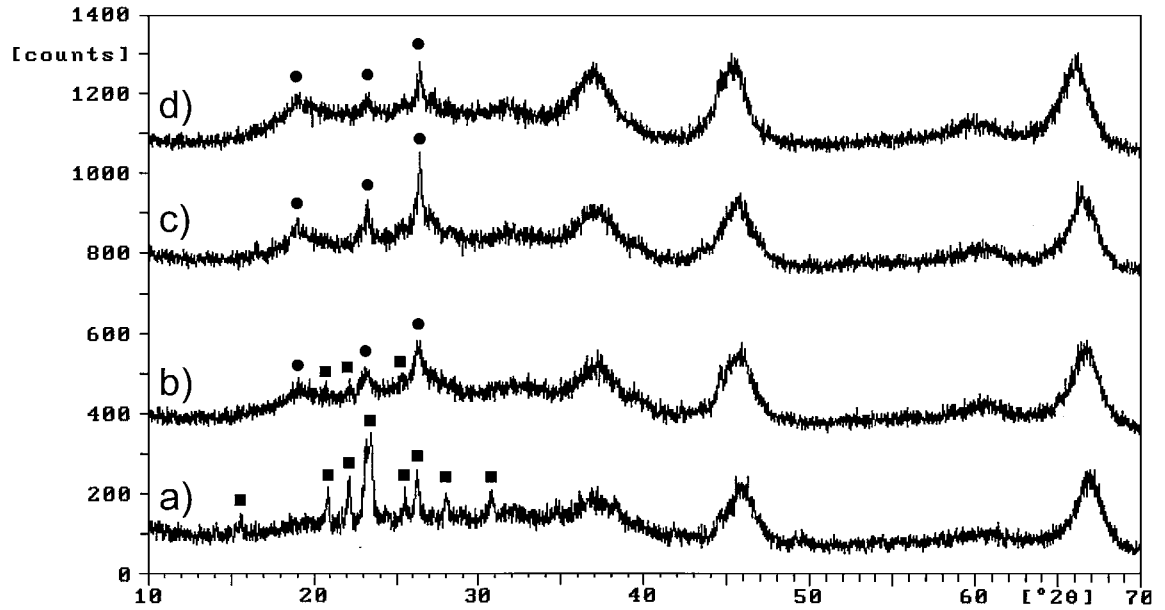

FIG. 2. X-ray diffractograms of the catalysts (a) Mo13Mg0.2, (b) Mo13Mg0.8, (c) Mo13Mg1.2, and (d) Mo13Mg2.9. The peaks are marked as (●) $MgMoO_4$ and (■) $Al_2(MoO_4)_3$.

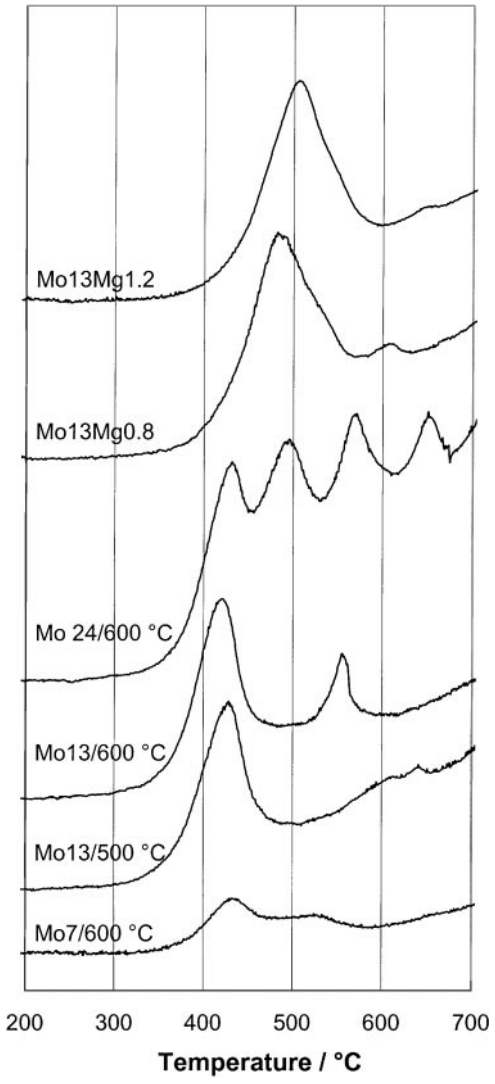

FIG. 3. TPR profiles of the catalysts to 700°C.

Oxidation States of Molybdenum

The TPR profiles of the catalysts are shown in Fig. 3. The TPR pattern of catalyst Mo13/600 contained two maxima: one at 422°C and the other at 556°C. The first maximum is related to the partial reduction of octahedrally coordinated molybdenum species in multilayers (23–26), while the second is related to the reduction of $Al_2(MoO_4)_3$ (25, 27). The new maximum in the TPR pattern of catalyst Mo24 indicates the reduction of crystalline MoO_3 at 495°C, as also reported by López Cordero *et al*. (23).

The TPR profiles of the catalysts containing both molybdenum and magnesium exhibited basically one maximum. The temperature of this maximum increased with magnesium content, from 462°C for a magnesium content of 0.8% (Mo13Mg0.2) to 544°C for a magnesium content of 8% (Mo13Mg2.9). The maximum is evidently composed of at least two peaks, which are related to the reduction of $MgMoO_4$ and molybdenum oxide species. The smaller peak at 607°C in the profile of Mo13Mg0.8 (see Fig. 3) may be related to the small amount of $Al_2(MoO_4)_3$ that was seen in the X-ray diffractogram.

The hydrogen consumption of the magnesium-containing catalysts was measured during temperature-programmed reduction between 30 and 560°C and is presented in Table 2. The average oxidation state of molybdenum species was calculated on the basis of hydrogen consumption by assuming that the fresh catalyst was totally in the oxidation state Mo^{6+} and that 1 mol of hydrogen consumed would mean the reduction of 1 mol of Mo^{6+} to Mo^{4+}. The average oxidation state was between +3.7 and +3.9 for all the catalysts containing 13% molybdenum.

To study the oxidation states of Mo on the Mo13Mg0.8 catalyst in detail, XPS was performed after calcination in air at 560°C and after reduction of 5, 30, and 120 min at 560°C. A reduction for 120 min at 700°C was also performed to reduce part of the molybdenum to its metallic state. The Mo 3*d* spectra are presented in Fig. 4 and an example of the peak deconvolution is shown in Fig. 5. Table 3 summarizes the results of the peak fitting. The three Mo 3*d* doublets with the highest binding energies (Mo $3d_{5/2}$ at 233.0, 231.9, and 230.0 eV) correspond to the oxidation states Mo^{6+} [MoO_3, $Al_2(MoO_4)_3$- or $MgMoO_4$-like species], Mo^{5+}, and isolated Mo^{4+} (28–31), respectively. The interpretation of the fourth doublet with a mean binding energy value of 228.9 eV is more speculative, it being either a paired double-bonded Mo^{4+} (rutile MoO_2) (32) or some oxidation state below Mo^{4+} (24, 28, 29, 33, 34). The average oxidation state calculated after 30 min reduction at 560°C was 4.3, 3.9, or 3.4 depending on whether the lowest oxidation state was Mo^{4+}, Mo^{3+}, or Mo^{2+}, respectively. These calculations and the TPR results indicate that on the catalyst surface a part of molybdenum has an oxidation state below Mo^{4+}. After reduction at 700°C the signals characteristic of metallic molybdenum appeared with the binding energy of Mo $3d_{5/2}$ at 227.7 eV (28, 29, 35).

TABLE 2

Hydrogen Consumption during TPR[a]

	Temperature of the maximum (°C)	H_2 consumption (μmol/$g_{catalyst}$)	H_2 consumption/ Mo (mol/mol)	Average oxidation state of Mo
Mo13/500	427	1497	1.08	3.8
Mo13/600	422, 556	1494	1.07	3.9
Mo13Mg0.2	462	1541	1.12	3.8
Mo13Mg0.8	485	1585	1.14	3.7
Mo13Mg1.2	500	1565	1.16	3.7
Mo13Mg1.9	540	1535	1.09	3.8
Mo13Mg2.9	544	1398	1.05	3.9

[a] The temperature was increased from 30 to 560°C and kept at 560°C for 30 min.

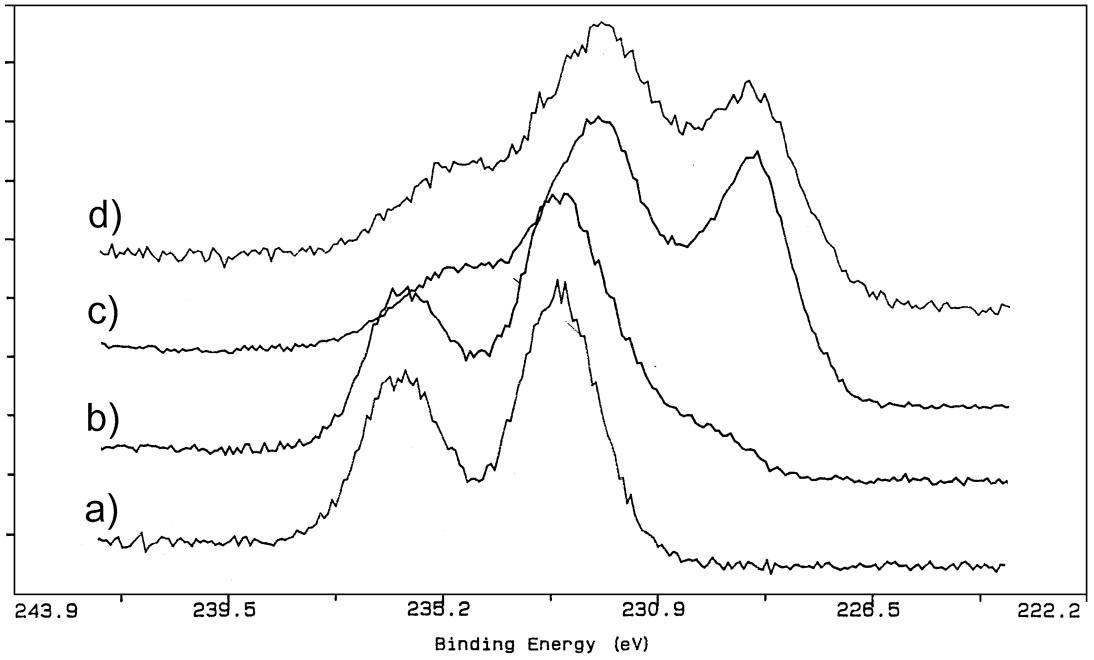

FIG. 4. Mo 3*d* photoelectron signals for catalyst Mo13Mg0.8 after (a) calcination in air and after reduction at 560°C in hydrogen for (b) 5, (c) 30, and (d) 120 min.

Activity

The thermal reactions of *n*-butane were studied in the absence of catalyst, with the volume of the catalyst bed replaced by an equal volume of carborundum. Under the conditions used for the activity tests the conversion of *n*-butane due to thermal reactions was less than 2%. The product mixture consisted of C_1–C_3 hydrocarbons.

The activity of the pure alumina support calcined at 600°C was tested in the reaction of *n*-butane and is shown in Fig. 6. The conversion of *n*-butane was 11% after 1 min on stream, and the selectivities to C_1–C_3 hydrocarbons and to

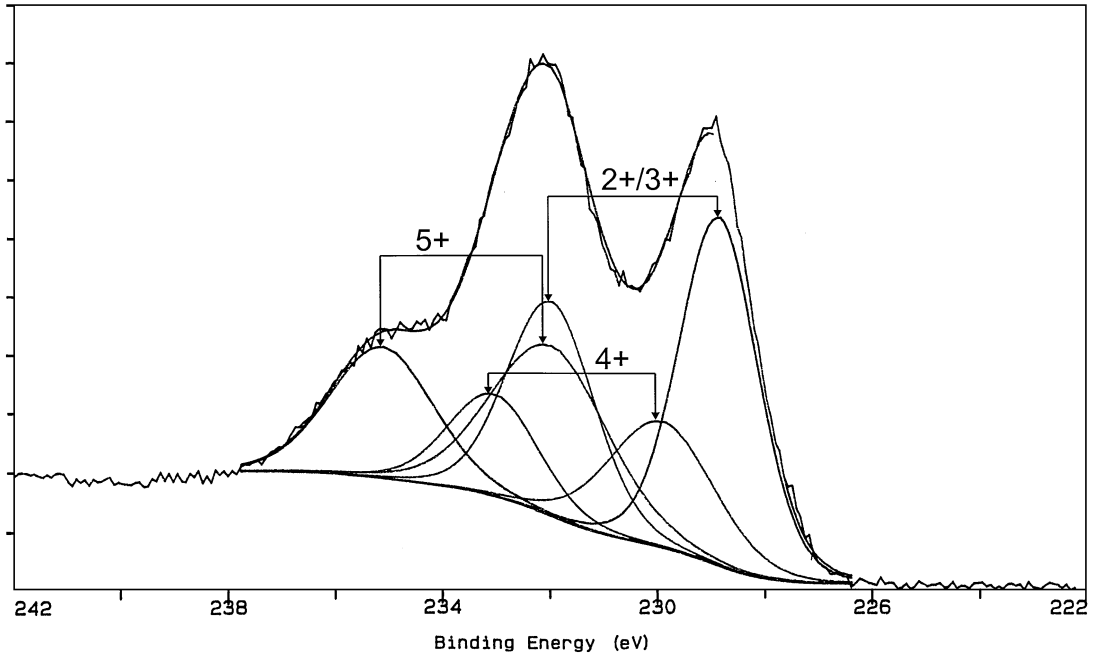

FIG. 5. Typical result (catalyst Mo13Mg0.8 reduced for 30 min at 560°C) of peak fitting procedure for Mo 3*d* signal.

TABLE 3

Results of Peak Deconvolution of the Mo 3*d* Photoelectron Signal for the Catalyst Mo13Mg0.8 after Calcination and after Reduction Periods of 5, 30, and 120 min at 560°C and 120 min at 700°C[a]

Catalyst Mo13Mg0.8	Mo $3d_{5/2}$	Mo $3d_{5/2}$	Mo $3d_{5/2}$	Mo $3d_{5/2}$	Mo $3d_{5/2}$
Calcined	232.9 eV				
no reduction	100%				
Reduction of	233.0 eV	231.8 eV	230.0 eV		
5 min at 560°C	63%	24%	13%		
Reduction of		232.0 eV	229.9 eV	228.9 eV	
30 min at 560°C		33%	22%	45%	
Reduction of		232.0 eV	230.1 eV	228.8 eV	
120 min at 560°C		36%	19%	45%	
Reduction of		231.8 eV	229.9 eV	228.7 eV	227.7 eV
120 min at 700°C		6%	21%	47%	26%
Oxidation state	Mo(VI)	Mo(V)	Mo(IV)	Mo(II,III)	Mo(0)

[a] Approximate fractions of oxidation states relative to total amount of Mo detected are shown.

all C_4 alkenes (1-butene, *cis*-2-butene, *trans*-2-butene, 1,3-butadiene, and i-butene) were 50 and 32%, respectively. The activity decreased during the first 3 min on stream, and the formation of C_1–C_3 products was reduced.

The conversions obtained with the MoO_x/alumina samples are shown in Fig. 6. The highest activity, where the conversion was 24% after 2 min on stream, was obtained with catalyst Mo13, which contained an amount of molybdenum closely corresponding to a theoretical monolayer on the alumina surface. The selectivity to all C_4 alkenes was only 49%, including the selectivity of 29% to *n*-butenes. The selectivity to C_1–C_3 hydrocarbons was 28%. The coke formed on the catalyst was not included in these calculations.

The product distribution in the test of Mo13 is shown in Fig. 7. The formation of CO, CO_2, and water during the first minutes on stream indicated the reduction of the molybdenum species by *n*-butane. The maximum yield of *n*-butenes, 7%, was obtained after 2 min on stream. The yield of 1,3-butadiene, approximately 4%, was highest during the first minute on stream and it decreased rapidly to 2%. The yields of C_1–C_3 hydrocarbons and i-butene increased to maxima of 7 and 3%, respectively, after 2 min on stream.

To increase the selectivity to *n*-butenes, the acidity of the alumina support was decreased by adding some magnesium (36, 37). The activity of the Mg/alumina sample was low, giving a conversion of *n*-butane less than 4% (Fig. 8). The main products formed were *n*-butenes and 1,3-butadiene, with a selectivity of 70%. No carbon oxides or i-butene was formed.

The activities of catalysts containing both molybdenum and magnesium during 10 min on stream are presented in Fig. 8. The conversion of *n*-butane decreased from 24 to 10–15% with the addition of magnesium. The conversion of *n*-butane and the selectivities after 2 min on stream are shown in Fig. 9. The magnesium increased the selectivity to all C_4 alkenes and lowered the selectivity to C_1–C_3 hydrocarbons. The selectivity to C_4 alkenes was highest (approximately 80%) for the catalyst containing 8% magnesium (Mo13Mg2.9).

The selectivity to heavier hydrocarbons, benzene and toluene, decreased with the addition of magnesium. For catalysts Mo13 and Mo13Mg2.9 the selectivities were 16 and 2%, respectively. The amount of coke formed on the catalyst during the dehydrogenation test followed the same trend, decreasing for the two catalysts from 3.1 to 0.3% (Table 4). If this coke formation were included in the carbon balance when calculating the catalyst activities, the conversion of *n*-butane would be higher and the selectivity to C_4 alkenes lower than those values presented in Fig. 9 (Table 4).

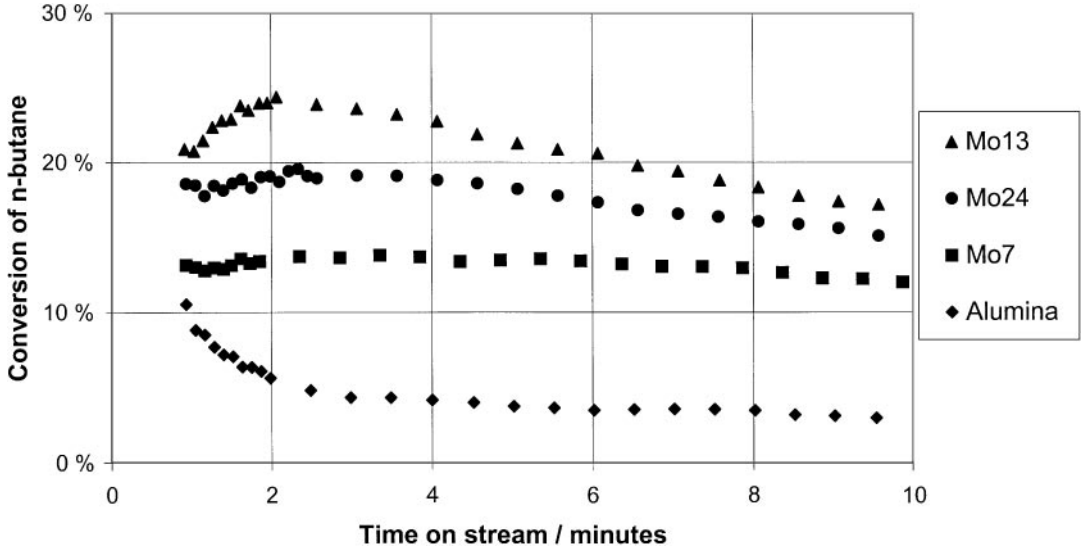

FIG. 6. Conversion of *n*-butane with MoO_x/alumina catalysts.

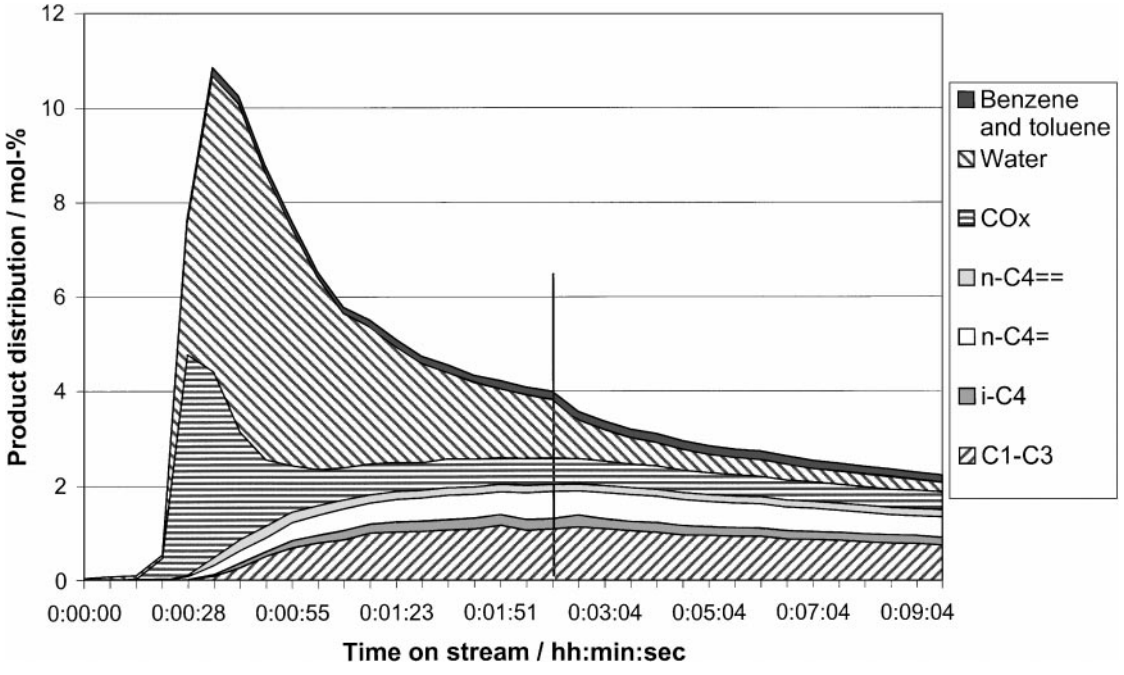

FIG. 7. Product distribution with the catalyst Mo13. The distribution was measured every 7 s during the first 2 min on stream and every 30 s after that.

Activity with Reduced Molybdenum Oxide Catalysts

To study the activity of the different oxidation states of molybdenum, the catalysts were reduced with hydrogen for 5 or 30 min before an activity test with *n*-butane. The results reported in Table 5 for catalysts Mo13 and Mo13Mg0.8 were obtained after 1 min on *n*-butane stream. For catalyst Mo13, the conversion of *n*-butane increased from 21 to 31 and 38% after prereductions of 5 and 30 min, respectively, while the selectivities to all C_4 alkenes decreased from 49 to 36 and 24%. After calcination the conversion of *n*-butane increased to a maximum of 24% and decreased slowly for 10 min (Fig. 8), whereas after the reduction periods the conversion fell off sharply. After calcination the selectivity to all C_4 alkenes was more or less stable at 50%, but the selectivity to 1,3-butadiene decreased and the selectivity to *n*-butenes increased with time. After a prereduction of 30 min the selectivity to C_4 alkenes increased from 24 to 38% and the selectivity to C_1–C_3 hydrocarbons decreased from 40 to 31%. The amount of coke formed on the catalysts during the test period increased when the catalysts were reduced with hydrogen before the test (Table 6),

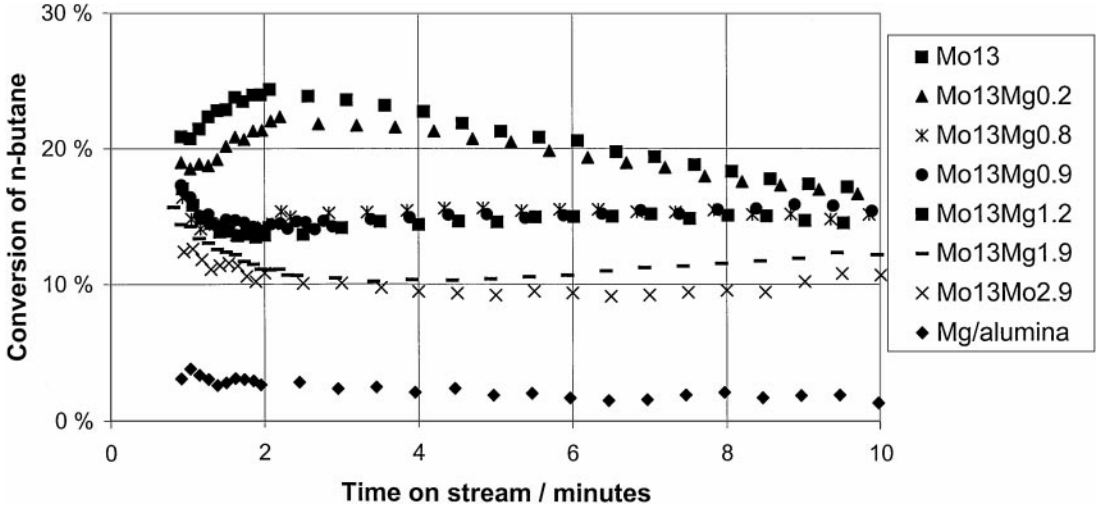

FIG. 8. Conversion of *n*-butane during 10 min on stream with catalysts containing both molybdenum and magnesium.

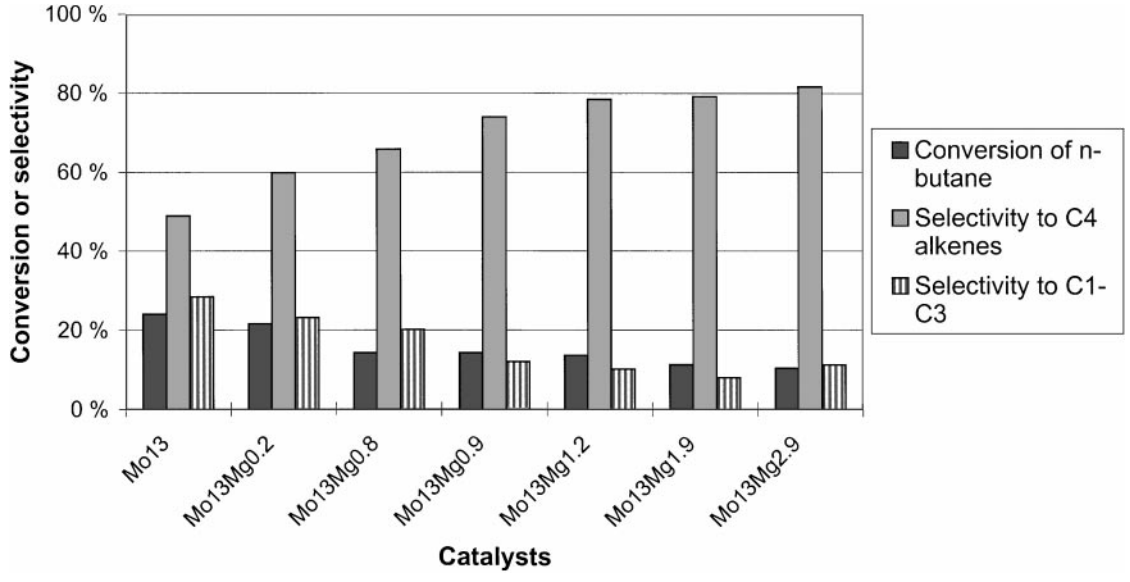

FIG. 9. Conversion of *n*-butane and selectivities after 2 min on stream with catalysts containing molybdenum and magnesium.

following the same trend as the conversion of *n*-butane.

During the activity test with *n*-butane, the reduction of molybdenum species was followed with a FTIR gas analyzer by measuring the oxygen compounds released from the catalyst. The assumptions made were that all the oxygen released originated from the catalyst, the molybdenum species on the fresh catalyst was completely in the Mo^{6+} state, and 1 mol of water, 1 mol of carbon monoxide or 0.5 mol of carbon dioxide released corresponded to the reduction of 1 mol of Mo^{6+} to Mo^{4+}. The average oxidation states of molybdenum species are presented in Table 7. In the calculation for hydrogen prereductions, the water and carbon oxides formed were divided into two parts. The first part is the amount of water detected during the reduction of the catalyst with hydrogen and the other is the water and carbon oxides released during the following activity test with *n*-butane. After 5 min hydrogen reduction, carbon dioxide was still formed under *n*-butane flow, indicating the further reduction of the molybdenum compounds. After hydrogen reduction of 30 min the oxidation state of the molybdenum species is assumed to be more or less stable, because during the following activity test hardly any carbon dioxide is formed. The water and carbon monoxide detected under *n*-butane flow were assumed to be formed mainly because of the retention of hydrogen in the catalyst during the previous hydrogen reduction (38).

TABLE 4

Carbon Content of the Catalyst after Dehydrogenation for 10 min and the Activities and Selectivities on Average during 10 min When the Carbon Content Is Included in the Carbon Balance

	Carbon content (%)	Conversion of *n*-butane	Selectivity to C_4 alkenes	Selectivity to coke
Mo13	3.1%	31	29	41
Mo13Mg0.2	2.4%	28	36	36
Mo13Mg0.8	1.6%	21	44	31
Mo13Mg0.9	1.4%	20	51	28
Mo13Mg1.2	1.2%	19	55	25
Mo13Mg1.9	0.7%	14	61	18
Mo13Mg2.9	0.3%	11	74	11

After 10 min on *n*-butane stream the average oxidation state of catalyst Mo13 was close to the value obtained after reduction with hydrogen for 5 min and with *n*-butane for 5 min. The same was observed for Mo24. The oxidation state of the magnesium-containing catalyst Mo13Mg0.8 was slightly lower than that without magnesium modification (Table 7).

To study the reduction of molybdenum compounds in detail, the formation of water is presented separately. Figure 10a shows the cumulative amount of water formed (A) during the activity test of catalyst Mo13. The amount of water assumed to be formed via reduction of molybdenum compounds with *n*-butane is presented with curve B. Curve B was calculated from carbon oxides released during reduction according to the following stoichiometry: $C_4H_{10} + (2x + 5/2)O_2 = 4CO_x + 5H_2O$. It is clear that the total amount of water detected during the activity test was higher than expected from reaction B and that the difference between the curves decreased during the test. For comparison, Fig. 10b shows that the amount of water released (A) after 5 min hydrogen prereduction was significantly lower than without the prereduction. In this case it is not possible to estimate the amount of water formed due to the catalyst reduction (B) because of hydrogen retention in

TABLE 5

Activity of the Catalysts Mo13 and Mo13Mg0.8 after 1 min on *n*-Butane Stream after Three Pretreatments

	Mo13			Mo13Mg0.8		
	Calcination	Reduction of 5 min with H_2	Reduction of 30 min with H_2	Calcination	Reduction of 5 min with H_2	Reduction of 30 min with H_2
Conversion of *n*-butane (%)	21	31	38	15	22	30
Selectivity to *n*-butenes (%)	26	20	13	22	34	21
Selectivity to 1,3-butadiene (%)	13	5	3	35	12	5
Selectivity to i-butene (%)	10	11	8	6	14	9
Selectivity to C_1–C_3 (%)	25	36	40	14	22	34
Selectivity to CO_x (%)	13	6	8	13	5	7
Selectivity to heavier hydrocarbons (%)	13	21	27	11	12	24

the catalyst. Figures 10a and 10b show also the cumulative amount hydrogen that should be released from C_4 alkenes formed from *n*-butane.

With catalysts containing both molybdenum and magnesium, the difference between curves A and B increased. The amount of carbon oxides released decreased and the amount of water formation increased with magnesium modification. However, the average oxidation state of molybdenum compounds calculated from the total amount of water and carbon oxides released during 10 min on *n*-butane stream was between 4.4 and 4.7 for all the catalysts containing 13% molybdenum.

Also, the ratio between 1,3-butadiene and *n*-butenes increased with magnesium modification. For catalysts Mo13, Mo13Mg0.8, and Mo13Mg2.9 this ratio was 0.5, 1.7, and 2.6 mol/mol, respectively, after 1 min on *n*-butane stream. After 30 min hydrogen reduction this ratio was 0.2, 0.2, and 0.5 mol/mol, respectively, for the same catalysts.

DISCUSSION

The reduction of molybdenum oxide on different supports has been studied widely, since reduction is essential during transformation of the oxide precursor to the sulfidic state (39). In most of these studies the temperature during calcination of the catalyst was below 550°C. We carried out calcination at 600°C because owing to thermodynamic limitations the temperature of the endothermic dehydrogenation reaction has to be above 550°C. Above 600°C, dehydrogenation selectivity diminishes due to thermal reactions.

With high molybdenum content, $Al_2(MoO_4)_3$ crystallites are formed during calcination at 550–600°C (23, 40–44). According to XRD, sample Mo13 contained crystalline MoO_3 after calcination at 500°C, but $Al_2(MoO_4)_3$ crystallites were formed at 600°C. These crystalline structures are typical of molybdenum loadings higher than the monolayer capacity of the alumina surface, but also around and even below the theoretical monolayer coverage (22, 45). After calcination at 600°C, MoO_3 crystallites are typically found only at higher molybdenum contents, as noted in our study with catalyst Mo24.

The average oxidation state of molybdenum obtained after reduction of the catalyst increased in the order Mo24 < Mo13 < Mo7 (Table 7). It is known that the reduction of molybdenum species on alumina is more difficult at low loadings (23). The molybdenum compounds in catalysts Mo13 were reduced, on average, to the same oxidation state both with *n*-butane (10 min) and with hydrogen/*n*-butane (5 + 5 min) reduction. The average oxidation state obtained after 30 min reduction with hydrogen (4.3) was close to the value of 3.9 obtained after TPR measurement (Table 2).

TABLE 6

Influence of Pretreatment on the Carbon Content of the Catalyst after Dehydrogenation

	Pretreatment		
	Calcination	Reduction of 5 min with H_2	Reduction of 30 min with H_2
Mo13	3.1%	3.0%	3.4%
Mo13Mg0.2	2.4%	2.5%	2.9%
Mo13Mg0.8	1.6%	2.1%	n.m.
Mo13Mg0.9	1.4%	2.1%	n.m.
Mo13Mg1.2	1.2%	1.5%	2.1%
Mo13Mg1.9	0.7%	1.0%	1.7%
Mo13Mg2.9	0.3%	0.4%	1.5%

TABLE 7

Average Oxidation State of Molybdenum Compounds Measured with an FTIR Gas Analyzer during Reduction with *n*-Butane or Hydrogen

	Mo7	Mo13	Mo24	Mo13Mg0.8
Reduction with *n*-butane for 10 min	5.4	4.7	4.4	4.4
Reduction with H_2 for 5 min	5.1	4.9	5.0	4.6
and with *n*-butane for 5 min	4.9	4.7	4.5	4.3
Reduction with H_2 for 30 min	4.7	4.6	4.2	4.2
and with *n*-butane for 5 min	4.6	4.3	4.0	4.0

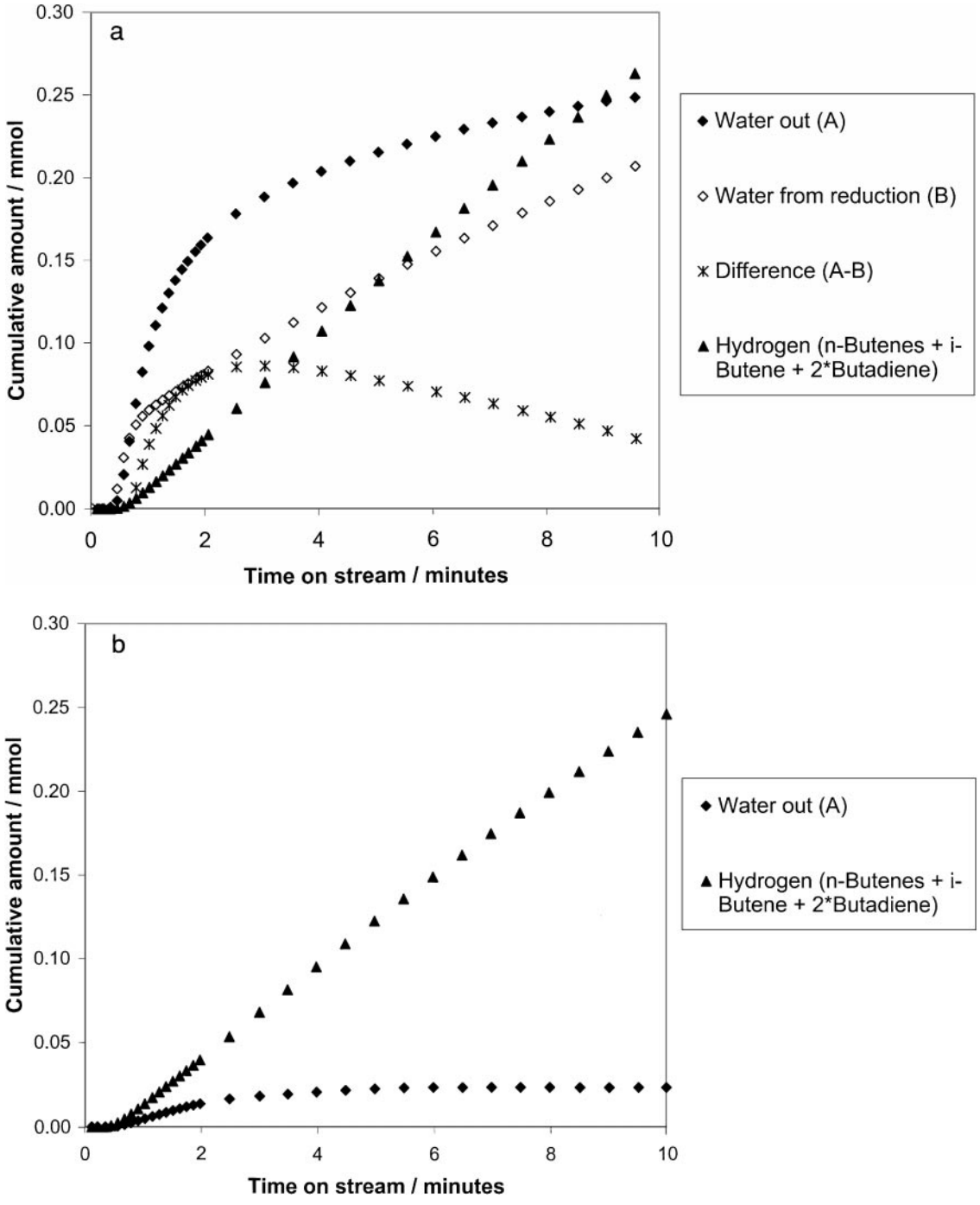

FIG. 10. (a) Water formation during the activity test after calcination with catalyst Mo13. (b) Water formation during activity test after 5 min hydrogen reduction with catalyst Mo13.

Influence of Magnesium Addition

Addition of magnesium to an amount Mg : Mo 1 : 1 mol/mol before impregnation of molybdenum prevented the formation of crystalline $Al_2(MoO_4)_3$. Instead, molybdenum and magnesium reacted to $MgMoO_4$ during the calcination at 600°C. These observations agree well with the results of Abello *et al.* (46) and Vrieland and Murchison (47).

According to TPR results the differences in the extent of reduction of the catalysts containing 13% molybdenum and 0 to 8% magnesium were small: the molybdenum species were reduced to an average oxidation state between +3.7 and +3.9 at 560°C. The reduction of the molybdenum

species took place at higher temperatures in the presence of magnesium. This can be partly due to the formation of crystalline $MgMoO_4$, but also the octahedrally coordinated molybdenum species and crystalline $Al_2(MoO_4)_3$ were reduced at higher temperatures. Mulcahy *et al.* (37) have shown that the modification of alumina with magnesium leads to an increase in the basicity of the support and in the number of hydroxyl groups and to increased dispersion of the molybdenum species. This could be one reason for higher reduction temperatures. Although the differences in the oxidation state were small, the lowest oxidation state was observed with catalysts Mo13Mg0.8 and Mo13Mg1.2, where the molar Mg : Mo ratio was close to 1 : 1. This observation was supported by the results obtained with the FTIR gas analyzer (Table 7).

The average oxidation states of molybdenum compounds obtained for catalyst Mo13Mg0.8 with different methods (TPR, FTIR, and XPS) were very close: the values measured after 30 min hydrogen reduction were 3.7 and 4.0 with TPR and FTIR, respectively, and 3.9 or 3.4 with XPS depending on the lowest oxidation state of molybdenum used in the calculation.

Active Sites

The activity of the alumina support under the conditions studied is most likely attributable to the acidic sites. The formation of cracked hydrocarbons from *n*-butane at these sites took place mostly during the first minutes on stream. The magnesium impregnated on the catalyst presumably also reacted with these sites, as seen in the much lower activity of the Mg/alumina than the alumina sample. In addition, the amount of coke formed on the Mg/alumina catalyst surface during the *n*-butane feed of 10 min was 1/20th what it was on alumina.

Two features were evident in the results of the activity tests. First, during the tests the molybdenum species were reduced by the hydrocarbons to lower oxidation states, with effects on both conversion and selectivity. Second, the yields of the various products decreased with time on *n*-butane stream at different rates. These features can be distinguished by comparing the results of the activity tests with and without the hydrogen reduction prior to the test. The possible influence of coke on the activity of the catalysts cannot be ruled out after several minutes on stream; therefore, we have concentrated our study on the initial activity of the catalysts.

When no prereduction with hydrogen was applied the selectivity to 1,3-butadiene was highest with every catalyst during the first minute on stream. During the same first minute, the yield of *n*-butenes increased to a maximum value and decreased slowly. After reduction with hydrogen the yield of 1,3-butadiene was low but stable during the 10-min test, and the yield of *n*-butenes remained high.

Comparison of the stoichiometric amounts of carbon oxides and water formed due to the reduction by the hydrocarbon and the total amount of water formed (Fig. 10a) during the activity test led us to conclude that part of the C_4 alkenes was formed by oxidative dehydrogenation reaction. The products formed via this reaction were 1,3-butadiene and water or *n*-butenes and water. During the first 4 min on *n*-butane stream, some other products were also formed from oxidative dehydrogenation; for example, the amount of benzene detected in the product was high during the first minutes.

After calcination the oxidation state of molybdenum was Mo^{6+}. The first products formed were carbon oxides and water. About 20 s later, C_4 alkenes and water (Difference, Fig. 10a) were detected in the product. The active species for oxidative dehydrogenation was most likely a reduced oxidation state of molybdenum, Mo^{5+} or Mo^{4+}, or a combination of the reduced oxidation state and Mo^{6+} (46, 47). During the test the rate of oxidative dehydrogenation decreased rapidly because of the limited amount of labile oxygen available on the catalyst (47). This interpretation is supported by the considerably lower yields of 1,3-butadiene and water obtained after the hydrogen prereduction.

After 5 min of hydrogen reduction (Fig. 10b), small amounts of water were formed by the further reduction of the catalyst by *n*-butane feed; at the same time the yield of *n*-butenes remained high. It was therefore, concluded, that at this stage *n*-butenes were formed via the dehydrogenation reaction, the products being *n*-butenes or 1,3-butadiene and hydrogen. Because the dehydrogenation activity also remained quite high after 30 min of H_2 reduction, the oxidation state Mo^{5+} or Mo^{4+} was most likely active in the dehydrogenation reaction.

The conversion of *n*-butane with the calcined catalyst Mo13 (Fig. 8) decreased slowly during the 10-min activity test. The conversion was higher after the prereductions but the activity declined fast. Since after 30 min prereduction the change in the average oxidation state during the test was minor, we concluded that this rapid decrease in activity was due to coke formation. After the 10-min test period (Table 6) the amount of coke was noticeably higher on the reduced than on the calcined catalyst. The yields of C_1–C_3 hydrocarbons followed the same trend as the coke formation: they were very low on the fresh catalyst and increased during the reduction of the catalyst with hydrocarbon and after the reduction with hydrogen. Several oxidation states could serve as the active sites for these reactions (Mo^{5+}, Mo^{4+}, $Mo^{3+/2+}$), but according to our results the most active would seem to be the lowest oxidation state, $Mo^{3+/2+}$. During the reduction of molybdenum species the Mo–O–Al bonds are broken, the alumina surface is uncovered, and the acidity of the catalyst surface is changed (22, 42, 48, 49). This, in turn, could lead to an increase in the selectivity to the cracked products and in coke formation on alumina.

Due to coke formation, however, the activity of the sites rapidly declines.

No i-butane was formed as a product of isomerization, so i-butene was assumed to be formed mainly through isomerization of *n*-butenes. The ratio of the yield of i-butene to that of *n*-butenes was between 0.2 and 0.4. The ratio increased after reduction with hydrogen and decreased with catalysts containing more molybdenum. These changes could be due to the differences in the acidic character of the catalyst samples (49).

Influence of Magnesium on Activity

The addition of magnesium increased the selectivity to *n*-butenes. The highest yield of *n*-butenes, 8%, was obtained after 5 min reduction with hydrogen for catalysts having a magnesium content of 3–4% and Mg : Mo molar ratio of approximately 1 : 1. Furthermore, the addition of magnesium reduced substantially the selectivity to heavier hydrocarbons, benzene and toluene. The amount of coke formed on the catalyst after calcination decreased from 3.1 to 0.3 wt% with the addition of 8 wt% magnesium. These observations can be explained by the reducing effect of magnesium on the acidity of the catalysts.

The magnesium modification also affected the reduction route of the catalysts. The molybdenum compounds were reduced with *n*-butane partly via a slow oxidative dehydrogenation reaction and partly via a reduction to carbon oxides and water. The selectivity toward oxidative dehydrogenation increased with magnesium addition. The average oxidation state of molybdenum compounds was, however, roughly the same after 10 min of *n*-butane independent of the magnesium content.

CONCLUSIONS

From the results of this study, we conclude that the active oxidation state of molybdenum for the dehydrogenation reaction is either Mo^{5+} or Mo^{4+}. This oxidation state was formed during reduction of molybdenum Mo^{6+} by hydrogen or by *n*-butane. However, this active oxidation state was not stable on the alumina carrier under the conditions used for testing, and the molybdenum compounds were reduced further to the lower oxidation states that were active in cracking of *n*-butane and coke formation.

The selectivity to C_4 alkenes was improved by modifying the catalyst with magnesium. The best yield of *n*-butenes, 8%, was obtained with the Mg : Mo molar ratio of 1 : 1. The highest selectivity to C_4 alkenes, 80%, was obtained with the highest amount of magnesium, because the selectivity was increased due to the oxidative dehydrogenation reaction.

The activity of the molybdenum catalyst and its selectivity for dehydrogenation were substantially lower than the activity and selectivity of chromium oxide on alumina. With chromium catalysts, the selectivity to C_4 alkenes is approximately 95% and the selectivities for oxidative dehydrogenation and isomerization are small.

ACKNOWLEDGMENTS

Support of this research by the Finnish Academy is gratefully acknowledged. We especially thank Mr. Asko Sneck at Neste Oy, Corporate Technology, for the SEM work, Ms. Erja Nykänen at Helsinki University of Technology for the XRD analyses, and Ms. Reetta Laitonen and Mr. Petri Kobylin at Helsinki University of Technology for measuring the activities of the catalyst samples.

REFERENCES

1. Buonomo, F., Sanfilippo, D., and Trifirò, F., *in* "Handbook of Heterogeneous Catalysis" (G. Ertl, H. Knözinger, and J. Weitkamp, Eds.), Vol. 5, p. 2140. VCH, Weinheim, 1997.
2. Kogan, S., Herskowitz, M., Woerde, H. M., and van der Oosterkamp, P. F., *in* "Proceedings of the DGMK Conference: C_4 Chemistry—Manufacture and Use of C_4 Hydrocarbons, Aachen, Germany, 1997" (W. Keim, B. Lücke, and J. Weitkamp, Eds.), p. 117.
3. Hakuli, A., Kytökivi, A., Krause, A. O. I., and Suntola, T., *J. Catal.* **161**, 393 (1996).
4. Ledoux, M. J., Pham-Huu, C., Meunier, F., Del Gallo, P., Krause, A. O. I., and Niemi, V., *in* "Programme of the 11th International Congress on Catalysis—40th Anniversary, Baltimore, 1996," p. Po-361.
5. Johnson, M. M., and Hepp, H. J., U.S. Patent 3,280,210 (1966).
6. Kovach, S. M., and Kmecak, R. A., Great Britain Patent 1,398,531 (1975).
7. Ghosh, A. K., Tanaka, K., and Toyoshima, I., *J. Catal.* **109**, 221 (1988).
8. Ghosh, A. K., Tanaka, K., and Toyoshima, I., *J. Catal.* **108**, 143 (1987).
9. Russel, A. S., and Stokes, J. J., *Ind. Eng. Chem.* **38**, 1071 (1946).
10. Lee, F. M., U.S. Patent 4,607,129 (1986).
11. Lee, F. M., U.S. Patent 4,644,089 (1987).
12. Clark, D. M., Tromp, P. J. J., and Arnoldy, P., U.S. Patent 5,220,092 (1993).
13. Ashmawy, F. M., *J. Appl. Chem. Biotechnol.* **27**, 137 (1977).
14. Eastman, A. D., U.S. Patent 4,327,238 (1982).
15. Eastman, A. D., U.S. Patent 4,371,730 (1983).
16. Martin, G. R., U.S. Patent 3,793,392 (1974).
17. Barri, S. A., Dave, D., and Young, D., European Patent 150,107 (1985).
18. Seiler, H. G., Sigel, H., and Sigel, A., "Handbook of Toxicity of Inorganic Compounds." Marcel Dekker, New York, 1988.
19. Haber, J., *in* "Handbook of Heterogeneous Catalysis" (G. Ertl, H. Knözinger, and J. Weitkamp, Eds.), Vol. 5, p. 2253. VCH, Weinheim, 1997.
20. Hakuli, A., Kytökivi, A., Lakomaa, E.-L., and Krause, A. O. I., *Anal. Chem.* **67**, 1881 (1995).
21. Williams, C. C., Ekerdt, J. G., Jehng, J.-M., Hardcastle, F. D., and Wachs, I. E., *J. Phys. Chem.* **95**, 8791 (1991).
22. Okamoto, Y., and Imanaka, T., *J. Phys. Chem.* **92**, 7102 (1988).
23. López Cordero, R., Gil Llambias, F. J., and López Agudo, A., *Appl. Catal.* **74**, 125 (1991).
24. Brito, J. L., and Laine, J., *J. Catal.* **139**, 540 (1993).
25. López Cordero, R., López Guerra, S., Fierro, J. L. G., and López Agudo, A., *J. Catal.* **126**, 8 (1990).
26. Arnoldy, P., Franken, M.C., Scheffer, B., and Moulijn, J. A., *J. Catal.* **96**, 381 (1985).
27. Thomas, R., van Oers, E. M., de Beer, V. H. J., Medema, J., and Moulijn, J. A., *J. Catal.* **76**, 241 (1982).
28. Yasumaru, J., Yamada, M., Houlla, M., and Hercules, D. M., *in* "Studies in Surface Science" (L. Guczi, F. Solymosi, and P. Tétényi, Eds.), Vol. 75, p. 1867. Budapest, 1992.

29. Yamada, M., Yasumaru, J., Houlla, M., and Hercules, D. M., *J. Phys. Chem*. **95**, 7037 (1991).
30. Ward, M. B., Lin, M. J., and Lunsford, J. H., *J. Catal.* **50**, 306 (1977).
31. Patterson, T. A., Carver, J. C., Leyden, D. E., and Hercules, D. M., *J. Phys. Chem*. **80**, 1700 (1976).
32. Grünert, W., Stakheev, A. Yu., Feldhaus, R., Anders, K., Shpiro, E. S., and Minachev, Kh. M., *J. Phys. Chem*. **95**, 1323 (1991).
33. Grünert, W., Stakheev, A. Yu., Feldhaus, R., Anders, K., Shpiro, E. S., and Minachev, Kh. M., *in* "Studies in Surface Science" (L. Guczi, F. Solymosi, and P. Tétényi, Eds.), Vol. 75, p. 1053. Budapest, 1992.
34. Redey, A., Goldwasser, J., and Hall, W. K., *J. Catal.* **113**, 82 (1988).
35. Park, H. K., Lee, J. K., Yoo, J. K., Ko, E. S., Kim, D. S., and Kim, K. L., *Appl. Catal.* **150**, 21 (1997).
36. Vrieland, G. E., Khazai, B., and Murchison, C. B., *Appl. Catal.* **134**, 123 (1996).
37. Mulcahy, F. M., Houalla, M., and Hercules, D. M., *J. Catal.* **139**, 72 (1993).
38. Hall, W. K., and Massoth, F. E., *J. Catal.* **34**, 41 (1974).
39. Topsøe, H., Clausen, B. S., and Massoth, F. E., "Hydrotreating Catalysis." Springer-Verlag, Berlin, 1996.
40. Zingg, D. S., Makovsky, L. E., Tischer, R. E., Brown, F. R., and Hercules, D. M., *J. Phys. Chem*. **84**, 2898 (1980).
41. Wei, Z., Jiang, S., Xin, Q., Sheng, S., and Xieng, G., *Catal. Lett.* **11**, 365 (1991).
42. O'Young, C.-L., Yang, C.-H., De Canio, S. D., Patel, M.-S., and Storm, D. A, *J. Catal.* **113**, 307 (1988).
43. Liu, D., Zhang, L., Yang, B., and Li, J., *Appl. Catal.* **105**, 185 (1993).
44. Said, A. A., *Thermochim. Acta* **236**, 93 (1994).
45. Grünert, W., Stakheev, A. Yu., Mörke, W., Feldhaus, R., Anders, K., Shpiro, E. S., and Minachv, Kh. M., *J. Catal.* **135**, 269 (1992).
46. Abello, M. C., Gomez, M. F., and Cadus, L. E., *Ind. Eng. Chem. Res.* **35**, 2137 (1996).
47. Vrieland, G. E., and Murchison, C. B., *Appl. Catal.* **134**, 101 (1996).
48. Segawa, K., and Millman, W. S., *J. Catal.* **101**, 218 (1986).
49. Suarez, W., Dumesic, J. A., and Hill, C. G., Jr., *J. Catal.* **94**, 408 (1985).